Published in final edited form as:
Methods. 2011 March ; 53(3): 187–193. doi:10.1016/j.ymeth.2010.12.012.

Evaluating Age-Associated Phenotypes in a Mouse Model of Protein Dyshomeostasis

Jin-Na Min[a,†] and **Cam Patterson**[a,b,*]

[a] McAllister Heart Institute, University of North Carolina, Chapel Hill, NC 27599, USA

[b] Departments of Medicine, Pharmacology, Cell and Developmental Biology, University of North Carolina Chapel Hill, NC 27599-7525

Abstract

Proteotoxicity caused by an imbalanced protein quality control surveillance system is believed to contribute to the phenotypes associated with aging as well as many neurodegenerative diseases. Understanding and monitoring the impact of proteotoxicity in these processes offers researchers keen insight into the biology of aging, as well as other conditions that share similar pathological etiologies. In this methods review we present various technical approaches that can be used to calculate and characterize the phenotypes associated with aging that are linked to increased proteotoxicity. Methods such as the measurement of oligomer protein expression and the capacity of proteasome function are useful tools in observing both aging phenotypes and neurodegenerative diseases, both of which share the phenomenon of impaired protein homeostasis.

Keywords

proteotoxicity; aging; neurodegenerative disease; Senescence-associated β-galactosidase activity; oxidative damage; 26S proteasome activity

1. Introduction

Proteotoxicity caused by misfolded and aggregated proteins is considered to be an underlying mechanism mediating the pathogenesis of late onset neurodegenerative diseases such as Alzheimer's diseases (AD), Parkinson's diseases (PD) and polyglutamine diseases [1,2]. These diseases are characterized by the expression of specific disease-associated proteins (such as Aβ, α-synuclein, tau, and huntingtin) which result in the formation of misfolded toxic proteins and protein aggregates [1]. This, in conjunction with the impairment of a protein degradation system that normally removes toxic nonfunctional proteins and organelles, greatly contribute to the exacerbation of these diseases [3,4]. Similar findings of accumulated damaged and misfolded proteins and inefficient protein degradation are also prevalent in the aging process.

[*]Address correspondence to: Cam Patterson, M.D., M.B.A, Director, Division of Cardiology and McAllister Heart Institute, University of North Carolina at Chapel Hill, 8200 Medical Biomolecular Research Building, Chapel Hill, NC 27599-7126Tel.: (919) 843-6477; Fax: (919) 966-1743; cpatters@med.unc.edu.
[†]Present address: Yale University School of Medicine, 333 Cedar St., New Haven, CT 06520, USA

The aging process is a highly complex progression consisting of both physiological and pathological steps involving the functional decline of most biological systems including DNA repair, telomere maintenance and protein turnover system [5,6]. Similar to the findings associated with neurodegenerative diseases, studies now support the theory that cellular malfunction caused by accumulation of damaged and misfolded proteins and impaired protein degradation is a major contributing factor in the aging process [7,8].

Considering the impact that suboptimal maintenance of protein homeostasis has on aging and neurodegenerative diseases, monitoring proteotoxicity in conjunction with the analysis of pathological phenotypes is a valuable approach for evaluating the progress of neurodegenerative disease as well as aging processes. Previously we reported on the importance of properly maintained protein homeostasis in aging using the CHIP deficient mouse model. CHIP (carboxyl terminus of Hsp70-interacting protein) is a ubiquitin ligase and molecular chaperone essential for many protein quality control processes within the cell [9-11]. Mice deficient in CHIP exhibit a shortened life span with a premature aging phenotype accompanied by a decline in protein quality control [12]. In this Methods review, we discuss the techniques used in our study to characterize accelerated aging and to monitor protein toxicity in our studies. Given the similarities in the pathologies associated with aging and neurodegenerative diseases, the techniques outlined in this review should be useful to researchers wishing to measure the progression and mechanics of both aging and other diseases associated with protein aggregates and decreased protein quality control. Most of data present here is adapted from our previously published report using the CHIP deficient mouse model [12].

2. Methods

Tissue samples used in all of the following methods are collected from mice of various ages (3, 6, 12, and 24 month old) in order to gain insight into the pathological and biochemical changes of various parameters over the course of normal and accelerated aging. Mice are euthanized with a CO_2 overdose followed by cervical dislocation and various tissues are extracted, weighed and prepared for storage by snap freezing in liquid nitrogen within 20 min following euthanasia. Tissue samples are stored at -80°C until needed. For statistical analysis, at least 3 mice per group (typically 5 animals per group) are used in each experiment.

2-1. Analyzing age-associated phenotypes in mouse models: anatomical and biochemical characteristics of aging

Studies of premature/accelerated aging in mammals commonly use anatomical and biochemical changes as an indicator of age-associated pathophysiological phenotypes [6,13]. In addition, a decrease in maximal lifespan without specific pathological features is another representative characteristic of an accelerated aging phenotype in mouse model systems [14]. Here we summarize the general methods used to identify age-associated phathophysiological changes in mouse models.

2-1-1. Longevity analysis: Kaplan-Meier survival curve—Median survival and maximum survival is a general but extremely useful determinant of changes in longevity. Although mice exhibit minor variations in longevity depending on genetic strain and gender, the average laboratory mouse can live up to 2-3 years when housed in a specific pathogen free (SPF) environment [15]. In the case of mortality related purely to normal aging, death is preceded by a generalized lack of movement and response to stimuli and difficulty of breathing, in the absence of any outward sign of diseases. Using GraphPad Prizm software, a Kaplan-Meier curve, which estimates survival fraction over time, is plotted and a logrank

test is performed to determine the significant difference in survival between the various groups tested. Figure 1 shows an example of the Kaplan-Meier survival curve obtained for 24 CHIP +/+ and 27 CHIP-/- female mice that were observed for more than 2 years in our laboratory. The result of the logrank test indicates that the survival of the two genetic groups is significantly different (p=0.0003).

2-1-2. Body composition analysis—Changes in body composition is a useful index for determining the progression of both aging and disease as it offers a more detailed insight into these processes than just changes in body weight alone. Body composition analysis includes monitoring the degree of body fat, lean tissue and bone density. Age is associated with a major change in body composition in the form of declined lean body mass [16-18]. Bone loss (measured by a decrease in bone density) is another indicator of the aging process and correlates with the progression of osteoporosis in human aging [19]. Body composition is measured by dual energy X-ray absorptiometry (DEXA) using a Lunar PIXImus densitometer (GE-Lunar Corp; Nagy, 2000 #150}. For this analysis, mice are anesthetized with pentobarbital (60 mg/kg) and subjected to scanning on a Lunar PIXImus densitometer. Data obtained from the PIXImus densitometer includes measurements of bone mineral content (BMC, g), bone mineral density (BMD, g/cm^2), % fat and % lean for individual animals. Another age-associated skeleton malformation is the progress of kyphosis, a lateral curvature of the spine [20]. Although severe hyperkyphosis can be observed without measurement, detailed degrees of thoracic kyphosis can be monitored using a radiographic Cobb's angle. The angle is calculated by drawing two lines in the thoracic curve at spinal levels T4 and T12. The resultant the angel between the intersecting perpendicular lines is defined as the Cobb's angle. A higher degree of Cobb's angle indicates a more severe form of kyphosis.

2-1-3. Evaluating skin atrophy—Skin consists of three layers, namely the epidermis, dermis and subcutaneous layers. The major age-associated phenotypes in skin are characterized by atrophic skin and poor wound healing. Although both the epidermis and dermis layers are known to become thinner with age, a reduced dermis layer is commonly used to monitor skin atrophy since the dermis is much thicker and therefore easier to analyze when it come to visualizing changes over time [21,22]. To calculate the thickness of the dermis layer of skin, a section of skin from the back of the mouse is removed and embedded in OCT compound and prepared for frozen histological analysis. Skin sections are stained for Hematoxlyin and eosin to visualize the various skin layers and micrographs collected for comparative analysis. The thicknesses of the dermis layer is measured in more than 10 different areas from one section to minimize inaccuracies due to local variations in layer thickness. At least 3 different mice per group are used for statistical analysis. Figure 2A illustrates an example image of skin sections taken from CHIP+/+ and CHIP-/- mice at 12 months of age. Histological skin sections of CHIP-/- mice exhibit a greater degree of dermal thinning compared to CHIP+/+ mice, indicating advanced skin atrophic features in CHIP-/- mice.

2-1-4 Cell proliferation assay: 3T9 protocol—Senescence refers to the distinctive and irreversible G1 growth arrest condition caused by diverse stressors such as DNA damage dysfunction in telomeres [23]. Cells undergoing senescence accumulate with age (owing to the age-related decline in renewability of cells;[24]) and these senescent cells are believed to contribute to the aging process. The most common way to monitor cellular senescence is to measure the ability of cell division during cellular passages in non-immortalized primary cells such primary mouse embryo fibroblasts (MEFs). After multiple passages, primary cells undergo senesensce and stop dividing. In addition, they undergo a change in morphology and physiological characteristics. Primary MEFs generated from mouse embryos at

embryonic day 13.5 according to standard protocols are used to measure proliferation assay using a 3T3 or 3T9 assay [25]. The 3T9 protocol is performed by plating cells at a density of 9×10^5 cells in 60-mm dishes. Cells are then replated after cell counts every third day (next passage) to maintain the same cell density. Population doublings (PDs) are determined by the following formula: $\log_2$ (number of cells harvested/number of cells seeded). PDs per passage can be plotted to compare the ability of cell proliferation in different passages and groups.

2-1-5. Senescence-associated β-galactosidase (SA-β-gal) activity assay in primary MEFs—Another way to measure senescence in cells is to monitor galactosidase activity in higher pH (pH 6). Lysosomal galactosidase activity is normally expressed in most cells and is usually optimally detected in an acidic environment (pH 4). However, in senescent cells and aging tissues (but not in quiescent and terminally differentiated cells) galactosidase activity can be histochemically detected at a more basic pH (pH 6;[26]). It is believed that an increase in lysosome number and activity during replicative senescence and organismal aging is the cause for galactosidase activity being able to be detected at a more basic pH [27] [28]. Galactosidase activity at pH 6, so called senescence-associated β-galactosidase (SA-β-gal) activity, is considered a biochemical indicator of the senescence process. SA-β-gal assays can be performed in vitro using primary MEFs at different passages as well as in vivo using tissues from mice of different ages. SA-β-gal activity in MEFs is measured by X-gal (5-bromo-4-chloro-3-indolyl-β-D-galactopyranoside) staining using a commercially available Senescence detection kit (BioVision). MEFs are grown in 12 or 24 well plates at different passages, washed with 1×PBS and fixed with 10% formaldehyde for 10 min at room temperature. Following washing, cells that are to be assayed for SA-β-gal activity are stained with the x-gal substrate solution overnight at 37°C. The following day, cells are washed with 1×PBS and photographed under light microscopy to reveal SA-β-gal staining. Quantification of X-gal positive cells is achieved by counting positive cells in 20 different fields at 400× magnification. SA-β-gal activity can also be measured in isolated tissue samples using the labeling procedure described above adapted for frozen section histochemistry, however it should be noted that some tissues (such as liver and spleen) can exhibit a high degree of background staining and this should be considered carefully to ensure accurate data interpretation [29]. For whole animal studies, kidney is a good tissue of choice in which to examine SA-β-gal activity. Figure 2B shows an example of SA-β-gal staining in CHIP-/- and CHIP+/+ MEFs at passage 8, which corresponds to a relatively late passage in primary MEFs and is therefore a good representation of aged cells. Representative pictures indicate a higher number of X-gal positive cells in CHIP-/-MEFs compared to CHIP+/+ MEFs at the same passages indicating cells from CHIP-/- mice senesence faster compared to cells from CHIP+/+ mice.

2-1-6. Measuring oxidative damage—Oxidative stress in conjunction with mitochondrial dysfunction has been linked to neurodegenerative diseases [30,31]. Oxidative stress induces cellular toxicity by free radical/reactive oxygen species, resulting in damage to cellular macromolecules including lipid, DNA and proteins. Increased oxidative stress and damaged biomolecules are also a hallmark of the aging phenotype [32,33]. There are several ways to detect the level of oxidative stress in cells and tissues including the measurement of oxidized protein levels, cellular redox potential and lipid oxidation. The presence and level of oxidized proteins (detection of protein carbonyl groups) can be measured by the Oxyblot system (Millipore). This simple immonoblotting-based system allows for the detection of carbonylated proteins in cells as well as tissue lysates by a reaction with 2,4-dinitrophenyl (DNP) hydrazine using an anti-DNP polyclonal antibody. Another way of monitoring the oxidative damage in a system is by measuring cellular redox potential. Cellular redox potential decreases with age and certain disease states due to an

increase in reactive oxygen species and can be monitored by balance between the reduced (GSH) and the oxidized (glutathione disulfide, GSSG) forms of glutathione. A decrease in GSH levels as well as an increase in the ratio of GSSG to GSH represent a lower redox potential and also indicate higher oxidative stress. The ratio of GSSG to GSH can be measured using a commercially GSH assay kit available from Cayman Chemical. Elevated levels of lipid oxidation is another marker for increased oxidative stress during aging. 8-isoprostane is a specific and abundant by-product of lipid peroxidation found in tissues and circulating plasma. Measuring the level of 8-isoprostane is a reliable way to detect lipid oxidation and therefore oxidative stress[34,35] and can be performed using a commercially available 8-isoprostane enzyme immunoassay kit (Cayman Chemical).

2-2. Monitoring changes in protein homeostasis *in vivo*

As mentioned previously, changes in protein homeostasis are common in normal aging, accelerated aging and in certain neurodegenerative diseases. Therefore, being able to monitor and compare this parameter in various experimental settings is advantageous in gaining insight into the progression of aging and disease states. Defects in the process and components of protein quality control systems, such as molecular chaperones and the protein degradation systems, increase with age and usually correlate with an increase in the deposition of damaged proteins and protein aggregates. These altered protein species are often times toxic to a cell, resulting in collapse of protein homeostasis with age and in disease states [36]. Therefore, evaluation of protein homeostasis within a system can be achieved by measuring both the accumulation of protein oligomers as well as the degree of proteasomal activity in a given cell or tissue. To monitor changes in protein homeostasis with age in our studies, we used two simple methods to measure the level of toxic oligomer proteins and proteasome activity from tissue lysates.

2-2-1. Detection of soluble oligomer proteins in tissue lysates using a commercially available anti-oligomer antibody—Soluble oligomer proteins are intermediate products of fibril-type aggregates. Despite the fact that they are soluble in nature, these oligomer proteins are known to cause higher cellular toxicity than larger fibril aggregates [37,38]. The toxicity of soluble oligomer proteins is particularly well recognized in Alzheimer's diseases associated with soluble Aβ peptides [39]. To measure the level of soluble oligomer proteins without sequence specificity, a specific antibody (A11, Biosource) has been developed which recognizes a common conformation-dependent structure present in all soluble oligomers [39]. Originally, this anti-oligomer anibody was only used to detect soluble Aβ oligomer proteins in AD samples, however the fact that this antibody probably recognizes a oligomeric conformation common to many different proteins (in addition to Aβ and small heat shock proteins), makes it difficult to interpret exactly which protein(s) are actually being detected in an experiment. Nevertheless, the A11 antibody is now widely utilized to determine general soluble oligomer proteins including Aβ oligomers, mutant α-B-crystallin in desmin-related cardiomyopathy models, and soluble polyQ proteins in cell culture system [40].

2-2-1-1 Preparation of soluble proteins from tissues: The detection of soluble oligomer proteins has been successfully achieved in cells as well as certain tissues including the brain and heart [39,41]. To extract soluble proteins from tissues, approximately 50mg to 100mg of the desired tissue is collected and lysed in 200ul to 400ul of 1×PBS containing a protease inhibitor (Roche) using pestle homogenizer. After removal of the insoluble proteins by centrifugation (15000g, 15min, 4°C), the concentration of soluble protein is measured using a Pierce® BCA Protein Assay Kit (Thermo Scientific). To avoid artificial protein aggregates and denaturation, all materials are kept on ice and the generation of heat and bubbles is minimized during tissue lysis.

2-2-1-2 Dot blot analysis to detect oligomer proteins: To detect the expression of soluble oligomer proteins, 10 to 20ug of soluble protein is loaded onto a nitrocellulose membrane (0.4μm pore size) and then dried for several hours to overnight at room temperature. Nonspecific labeling is blocked by incubating membranes with 5% (w/v) nonfat dry milk in TBS containing 0.025% Tween 20 (TBST) overnight at 4°C. The A11 anti-oligomer antibody (Biosource) is diluted in 3% (w/v) nonfat dry milk-TBST to a concentration of 1ug/ml and the membrane with bound soluble oligomer proteins is incubated for 2 hours at room temperature or overnight at 4°C. The membrane is subsequently incubated with a secondary antibody (HRP conjugated goat anti-rabit IgG, 1:5000 dilution) in 3% (w/v) nonfat dry milk -TBST for 1 hour at room temperature. Between incubations, membranes are washed 3 times with TBST. Following the last wash, the membrane is exposed to x-ray film and developed using an Amersham ECL Plus™ Western Blotting Detection Reagents (GE Healthcare). A positive control of purified α-B-crystallin (R120G) recombinant protein, known for its ability to form soluble oligomers, is used for this assay [40]. In order to ensure loading accuracy, soluble proteins are denatured by adding SDS (to a final concentration of 1%) and heated at 95°C for 5 min. Denatured proteins are then loaded onto a nitrocellulose membrane, incubated with an anti-α-actin antibody and processed using the same procedure as describe. Figure 3A demonstrates the age-associated increase in expression of soluble oligomer proteins in mouse brain using dot bot analysis. Consistent with the hypothesis that CHIP-/- mice undergo accelerated aging, brain extracts from CHIP-/- mouse express more abundant soluble oligomer proteins compared to the brain extract from age-matched wild type mice. Figure 3B demonstrates the dot blot result from a positive (a purified protein of mutant α-B-crystallin, R120G) and negative (a purified protein of wild-type α-B-crystallin) control for anti-oligomer antibody.

2-2-2. Measuring 26S proteasome activity using fluorogenic substrates—The ubiquitin proteasome system (UPS) represents one of the major proteolytic systems used by cells to degrade damaged or worn cytosolic, endoplasmic reticulum, and nuclear proteins via the 26S proteasome. UPS dysfunction has been linked to the pathogenesis of several neurodegenerative diseases as well as the aging process [1,42-44]. In addition, 26S proteasome activity can be compromised by several conditions such as an overload of substrates including misfolded proteins and aggregates [45]. Other circumstance such as energy deficit, decreased expression of proteasome subunits, and stress condition are also known to contribute to defects in 26S proteasome activity [7,46]. The 26S proteasome consist of a central catalytic core complex called the 20S unit and two 19S regulatory units [47,48]. The 20S catalytic core complex also contains six peptidase sites: two chymotrypsin-like, two caspase-like and two trypsin-like sites. Although the 20S core itself can exist as a free form unit (which is actually more stable than the 26S complex), studies suggest that only the 26S proteasome plays a critical role in protein degradation since the 20S proteasome is not able to degrade intracellular proteins or polyubiquitinated proteins under physiological conditions. Proteolysis via the 26S proteasome is an ATP dependent process, which is another distinguishing feature that sets it apart from the 20S proteasome [49]. The specific activity of each peptidase within the 26S proteasome can be determined in tissue lysates using a fluorophore (7-amino-4-methylcoumarin, AMC)-conjugated specific peptide substrate and the kinetic assay described below [50]. Since all three peptidase activities reflect 26S proteasome function, the activity of all sites needs to be monitored to evaluate the capacity of proteasome. It bears noting that this assay involves using fluorogenic peptide substrates that consist of few peptides, and hence are considerably less complex than the native protein entities with which the 26S proteasome would usually deal. As such, even when there are no detectable defects in this assay there may still be other defects that go unnoticed that would be noticeable had the substrate been more complex in nature (for example entire ubiquitinated proteins that need to be unfolded before proteolysis can occur).

Nonetheless, measuring peptidase activity in this way is useful for determining 26S proteasome activity as long as the limitations of this assay are kept in mind when interpreting data.

2-2-2-1 Preparation of tissue lysates for 26S proteasome assay: To prepare crude tissue lysates for a proteasome activity assay, tissues (a minimum of 50 to 100 mg of tissues) are homogenized in a lysis buffer (250 mM sucrose, 50 mM Tris, pH 7.5, 5 mM $MgCl_2$, 0.5 mM EDTA, 1 mM dithiothreitol) to which 5mM ATP and 0.025% Digitonin are added immediately before use. The addition of ATP is necessary in order to distinguish 26S proteasome activity from 20S proteasome. Tissue homogenates are incubated in 4°C for 10 min for maximum lysis by digitonin and are then centrifuged (15000g, 15min at 4°C) to obtain soluble tissue lysates for the assay. Protein concentration is measured by the BCA method and tissue lysates are stored at -80°C until needed for assay analysis. To avoid alteration in proteasome activity by frequent freezing and thawing cycles, tissue lysates should be aliquoted into several tubes.

2-2-2-2 Kinetics assay for peptidase activities in tissue lysates: To measure the activity of each peptidase in the 26S proteasome, 20 to 30 ug of tissue protein extract (in the case of skeletal muscle and liver) are added to the proteasome reaction buffer (50 mM Tris, pH 7.5, 40 mM KCl, 1 mM $MgCl_2$, 1 mM dithiothreitol, 0.5 mM ATP, and 0.05 mg/ml bovine serum albumin) to which DTT, ATP, and albumin are added immediately before the start of the assay. Appropriate protein amounts need to be determined for each different tissue studied due to the variation in proteasome activity between tissues. Fluorogenic substrates purchased from Biomol (75μM of Suc-LLVY-AMC for Chymotrypsin-like activiy; 150μM of Boc-LRR-AMC for Trypsin-like activiy; 75μM of Ac-nLPnLD-AMC for Caspase-like activity) are diluted in the proteasome reaction buffer and pre-warmed at 37°C for 10 min before adding to tissue lysates. Fluorescence is measured every 2 min at 37°C for 80 minutes using a Wallace Victor2 Spectrofluorometer (the excitation wavelength is 355 nm, and the emission wavelength is 460 nm). To remove nonspecific substrate hydrolysis, another set of proteins is pre-incubated with the proteasome inhibitor epoxomycin (20 μM final concentration, Biomol) for 30 min at 37°C before adding the fluorogenic substrates and fluorescence units are subtracted from each measurement. Linear regression (GraphPad Prizm 4) is calculated by fluorescence unit (AFU/ug protein) and time (min) and the slope (AFU/min) of linear regression analysis is used for the comparison of peptidase activity. Each sample is assayed in triplicate and the average of triplicate measurement is used for linear regression analysis. Only slopes with good linearity ($R^2 > 0.95$) are used and the data from at least 3 different mice are subjected to statistical analysis (student *t*-test). This assay uses results obtained by continuous assay based on linearity as opposed to data obtained from an endpoint analysis. Endpoint analysis obtains data from one time point. This form of analysis is simple and often used in these types of assays. However, endpoint analysis allows the possibility of detecting saturated and inaccurate activity due to limited substrate availability in the reaction. In addition, in this particular assay, 26S proteasome subunits and activity can vary between samples even if they are at the same protein concentration [46]. Measuring peptidase activity via a continuous assay by calculating linear regression affords the ability to detect activity throughout the assay. As such, it allows the opportunity to exclude time points where saturated activities are obvious due to the exhaustion of substrates or higher 26S proteasome activity in certain samples, making the analysis of the data significantly more accurate. Figure 4A indicates representative kinetics assay from our previous studies using skeletal muscle analyzed for chymotrysin-like, trypsin-like and caspase-like activites. Figure 4B indicates reduced chymotrypsin-like activity in liver tissue from CHIP-/- mouse at 12-month old compared to that from age-matched CHIP+/+ mouse. Using this assay we demonstrated decreases in 26S proteasome activity in CHIP-/- mouse associated with their premature aging phenotype (Fig 4B).

3. Concluding remarks

There is a growing body of evidence suggesting that maintenance of protein homeostasis is a key regulatory mechanism in determining the speed of the aging process as well as the development of diseases linked to proteotoxicity such as neurodegenerative diseases [4,8]. Proteotoxicity is mediated by the accumulation of either toxic disease-specific proteins (for example Aβ protein in AD and huntingtin in Huntington's disease) or a broader range of misfolded/altered protein species (for example in the aging process). In addition, impairment of protein degradation systems such as the UPS and autophagy system contribute to the induction of proteotoxicity during the aging process as well as neurodegenerative diseases [1,7]. In this Methods review, we have presented a diverse range of techniques that we used in our study of the evaluation of the aging phenotype in a mouse model of protein dyshomeostasis [12]. Most of the techniques we cover (including measurement of soluble oligomer production, proteasomal activity, oxidative assays and proliferation assays) can also be attributed to studies involving the progression of neurodegenerative diseases.

Acknowledgments

We are thankful to Monte Willis (MD, PhD) for providing skeletal muscle samples for the proteasome activity assay. We also appreciate Andrea L. Portbury (PhD) for critical reading and editing of this manuscript.

Funding: This work was partially supported by National Institutes of Health grants GM61728 to CP.

References

1. Gray DA, Tsirigotis M, Woulfe J. Ubiquitin, Proteasomes, and the Aging Brain. Sci Aging Knowl Environ 2003;2003:re6.
2. Ross CA, Poirier MA. What is the role of protein aggregation in neurodegeneration? Nat Rev Mol Cell Biol 2005;6:891–898. [PubMed: 16167052]
3. Bence NF, Sampat RM, Kopito RR. Impairment of the Ubiquitin-Proteasome System by Protein Aggregation. Science 2001;292:1552–1555. [PubMed: 11375494]
4. Ross CA, Pickart CM. The ubiquitin-proteasome pathway in Parkinson's disease and other neurodegenerative diseases. Trends in Cell Biology 2004;14:703–711. [PubMed: 15564047]
5. Kirkwood TBL. Understanding the Odd Science of Aging. Cell 2005;120:437–447. [PubMed: 15734677]
6. Hasty P, Campisi J, Hoeijmakers J, van Steeg H, Vijg J. Aging and Genome Maintenance: Lessons from the Mouse? Science 2003;299:1355–1359. [PubMed: 12610296]
7. Tonoki A, Kuranaga E, Tomioka T, Hamazaki J, Murata S, Tanaka K, Miura M. Genetic Evidence Linking Age-Dependent Attenuation of the 26S Proteasome with the Aging Process. Mol Cell Biol 2009;29:1095–1106. [PubMed: 19075009]
8. Lindner AB, Demarez A. Protein aggregation as a paradigm of aging. Biochimica et Biophysica Acta (BBA) - General Subjects 2009;1790:980–996.
9. Ballinger CA, Connell P, Wu Y, Hu Z, Thompson LJ, Yin LY, Patterson C. Identification of CHIP, a Novel Tetratricopeptide Repeat-Containing Protein That Interacts with Heat Shock Proteins and Negatively Regulates Chaperone Functions. Mol Cell Biol 1999;19:4535–4545. [PubMed: 10330192]
10. Dai Q, Zhang C, Wu Y, McDonough H, Whaley RA, Godfrey V, Li HH, Madamanchi N, Xu W, Neckers L, Cyr D, Patterson C. CHIP activates HSF1 and confers protection against apoptosis and cellular stress. EMBO J 2003;22:5446–5458. [PubMed: 14532117]
11. Miller VM, Nelson RF, Gouvion CM, Williams A, Rodriguez-Lebron E, Harper SQ, Davidson BL, Rebagliati MR, Paulson HL. CHIP Suppresses Polyglutamine Aggregation and Toxicity In Vitro and In Vivo. J Neurosci 2005;25:9152–9161. [PubMed: 16207874]

12. Min JN, Whaley RA, Sharpless NE, Lockyer P, Portbury AL, Patterson C. CHIP Deficiency Decreases Longevity, with Accelerated Aging Phenotypes Accompanied by Altered Protein Quality Control. Mol Cell Biol 2008;28:4018–4025. [PubMed: 18411298]
13. Kalu, DN. Handbook of Physiology. Oxford Univ. Press; New York: 1995.
14. Kipling D, Davis T, Ostler EL, Faragher RGA. What Can Progeroid Syndromes Tell Us About Human Aging? Science 2004;305:1426–1431. [PubMed: 15353794]
15. Rong Y, Shirng-Wern T, Stefka BP, Caralina Marin de E, Shuqin X, Michael AM, Molly AB, Kevin DM, Luanne LP, Carol JB, Clifford JR, John PS, David EH, Gary AC, Beverly P. Aging in inbred strains of mice: study design and interim report on median lifespans and circulating IGF1 levels. Aging Cell 2009;8:277–287. [PubMed: 19627267]
16. Visser M, Pahor M, Tylavsky F, Kritchevsky SB, Cauley JA, Newman AB, Blunt BA, Harris TB. One- and two-year change in body composition as measured by DXA in a population-based cohort of older men and women. J Appl Physiol 2003;94:2368–2374. [PubMed: 12598481]
17. Sobel H, Hrubant HE, Hewlett MJ. Changes in the Body Composition of C57BL/6-aa Mice With Age. Journal of Gerontology 1968;23:387–389. [PubMed: 5663616]
18. O'Connor TP, Lee A, Jarvis JUM, Buffenstein R. Prolonged longevity in naked mole-rats: age-related changes in metabolism, body composition and gastrointestinal function. Comparative Biochemistry and Physiology - Part A: Molecular & Integrative Physiology 2002;133:835–842.
19. Geoffroy V, Kneissel M, Fournier B, Boyde A, Matthias P. High Bone Resorption in Adult Aging Transgenic Mice Overexpressing Cbfa1/Runx2 in Cells of the Osteoblastic Lineage. Mol Cell Biol 2002;22:6222–6233. [PubMed: 12167715]
20. Kado DM, Prenovost K, Crandall C. Narrative Review: Hyperkyphosis in Older Persons. Annals of Internal Medicine 2007;147:330–338. [PubMed: 17785488]
21. Makrantonaki E, Zouboulis C. Molecular Mechanisms of Skin Aging. Annals of the New York Academy of Sciences 2007;1119:40–50. [PubMed: 18056953]
22. Fisher GJ, Wang Z, Datta SC, Varani J, Kang S, Voorhees JJ. Pathophysiology of Premature Skin Aging Induced by Ultraviolet Light. New England Journal of Medicine 1997;337:1419–1429. [PubMed: 9358139]
23. Goldstein S. Replicative senescence: the human fibroblast comes of age. Science 1990;249:1129–1933. [PubMed: 2204114]
24. Campisi J. Senescent Cells, Tumor Suppression, and Organismal Aging: Good Citizens, Bad Neighbors. Cell 2005;120:513–522. [PubMed: 15734683]
25. Todaro GJ, Green H. Quantitative Studies of the Growth of Mouse Embryo Cells in Culture and Their Development into Established Lines. The Journal of Cell Biology 1963;17:299–313. [PubMed: 13985244]
26. Dimri GP, Lee X, Basile G, Acosta M, Scott G, Roskelley C, Medrano EE, Linskens M, Rubelj I, Pereira-Smith O, Peacocke M, Campisi J. A Biomarker that Identifies Senescent Human Cells in Culture and in Aging Skin in vivo. PNAS 1995;92:9363–9367. [PubMed: 7568133]
27. Lee BY, Han JA, Im JS, Morrone A, Johung K, Goodwin EC, Kleijer WJ, DiMaio D, Hwang ES. Senescence-associated β-galactosidase is lysosomal β-galactosidase. Aging Cell 2006;5:187–195. [PubMed: 16626397]
28. Kurz DJ, Decary S, Hong Y, Erusalimsky JD. Senescence-associated (beta)-galactosidase reflects an increase in lysosomal mass during replicative ageing of human endothelial cells. J Cell Sci 2000;113:3613–3622. [PubMed: 11017877]
29. Krishnamurthy J, Torrice C, Ramsey MR, Kovalev GI, Al-Regaiey K, Su L, Sharpless NE. Ink4a/Arf expression is a biomarker of aging. J Clin Invest 2004;114:1299–1307. [PubMed: 15520862]
30. Simonian NA, Coyle JT. Oxidative Stress in Neurodegenerative Diseases. Annual Review of Pharmacology and Toxicology 2003;36:83–106.
31. Trushina E, McMurray CT. Oxidative stress and mitochondrial dysfunction in neurodegenerative diseases. Neuroscience 2007;145:1233–1248. [PubMed: 17303344]
32. Bokov A, Chaudhuri A, Richardson A. The role of oxidative damage and stress in aging. Mechanisms of Ageing and Development 2004;125:811–826. [PubMed: 15541775]
33. Johnson FB, Sinclair DA, Guarente L. Molecular Biology of Aging. Cell 1999;96:291–302. [PubMed: 9988222]

34. Wang B, Zhu H, Sun H, Pan J, Yuan Z, Yu R. Plasma 8-Isoprostane Concentrations in Patients with Age-Related Cataracts. Clin Chem 2005;51:1541–1544. [PubMed: 16040854]
35. Roberts LJ, Morrow JD. Measurement of F2-isoprostanes as an index of oxidative stress in vivo. Free Radical Biology and Medicine 2000;28:505–513. [PubMed: 10719231]
36. Hipkiss AR. Accumulation of altered proteins and ageing: Causes and effects. Experimental Gerontology 2006;41:464–473. [PubMed: 16621390]
37. Bucciantini M, Giannoni E, Chiti F, Baroni F, Formigli L, Zurdo J, Taddei N, Ramponi G, Dobson CM, Stefani M. Inherent toxicity of aggregates implies a common mechanism for protein misfolding diseases. Nature 2002;416:507–511. [PubMed: 11932737]
38. Hardy J, Selkoe DJ. The Amyloid Hypothesis of Alzheimer's Disease: Progress and Problems on the Road to Therapeutics. Science 2002;297:353–356. [PubMed: 12130773]
39. Kayed R, Head E, Thompson JL, McIntire TM, Milton SC, Cotman CW, Glabe CG. Common Structure of Soluble Amyloid Oligomers Implies Common Mechanism of Pathogenesis. Science 2003;300:486–489. [PubMed: 12702875]
40. Sanbe A, Yamauchi J, Miyamoto Y, Fujiwara Y, Murabe M, Tanoue A. Interruption of CryAB-Amyloid Oligomer Formation by HSP22. J Biol Chem 2007;282:555–563. [PubMed: 17092938]
41. Sanbe A, Osinska H, Villa C, Gulick J, Klevitsky R, Glabe CG, Kayed R, Robbins J. Reversal of amyloid-induced heart disease in desmin-related cardiomyopathy. Proceedings of the National Academy of Sciences 2005;102:13592–13597.
42. Kristiansen M, Deriziotis P, Dimcheff DE, Jackson GS, Ovaa H, Naumann H, Clarke AR, van Leeuwen FWB, Menendez-Benito V, Dantuma NP, Portis JL, Collinge J, Tabrizi SJ. Disease-Associated Prion Protein Oligomers Inhibit the 26S Proteasome. Molecular Cell 2007;26:175–188. [PubMed: 17466621]
43. Wang J, Wang CE, Orr A, Tydlacka S, Li SH, Li XJ. Impaired ubiquitinâ€“proteasome system activity in the synapses of Huntington's disease mice. The Journal of Cell Biology 2008;180:1177–1189. [PubMed: 18362179]
44. Vernace VA, Arnaud L, Schmidt-Glenewinkel T, Figueiredo-Pereira ME. Aging perturbs 26S proteasome assembly in Drosophila melanogaster. FASEB J. 2007 fj.06-6751com.
45. Ciechanover A, Brundin P. The Ubiquitin Proteasome System in Neurodegenerative Diseases: Sometimes the Chicken, Sometimes the Egg. Neuron 2003;40:427–446. [PubMed: 14556719]
46. Keller JN, Gee J, Ding Q. The proteasome in brain aging. Ageing Research Reviews 2002;1:279–293. [PubMed: 12039443]
47. Baumeister W, Walz J, Zühl F, Seemüller E. The Proteasome: Paradigm of a Self-Compartmentalizing Protease. Cell 1998;92:367–380. [PubMed: 9476896]
48. Kisselev AF, Callard A, Goldberg AL. Importance of the Different Proteolytic Sites of the Proteasome and the Efficacy of Inhibitors Varies with the Protein Substrate. Journal of Biological Chemistry 2006;281:8582–8590. [PubMed: 16455650]
49. Coux O, Tanaka K, Goldberg AL. Structure and Functions of the 20S and 26S Proteasomes. Annual Review of Biochemistry 1996;65:801–847.
50. Kisselev, AF.; Goldberg, AL.; Raymond, JD. Methods in Enzymology. Vol. 398. Academic Press; 2005. p. 364

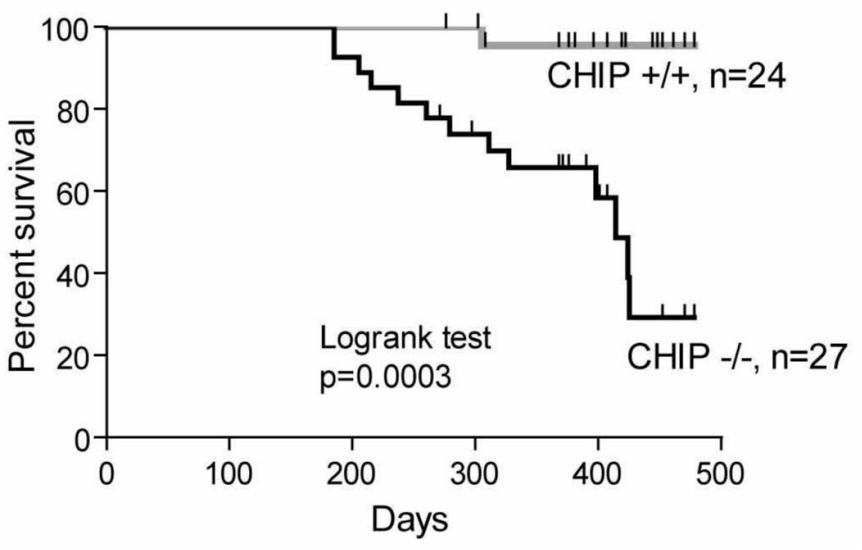

Figure 1. Kaplan-Meier survival curve

A Kaplan-Meier survival analysis in a cohort of female CHIP+/+ (n=24) and CHIP-/- mice (n=27). CHIP-/- mice have a significantly shortened lifespan compared with CHIP+/+ mice (Logrank test, p=0.0003).

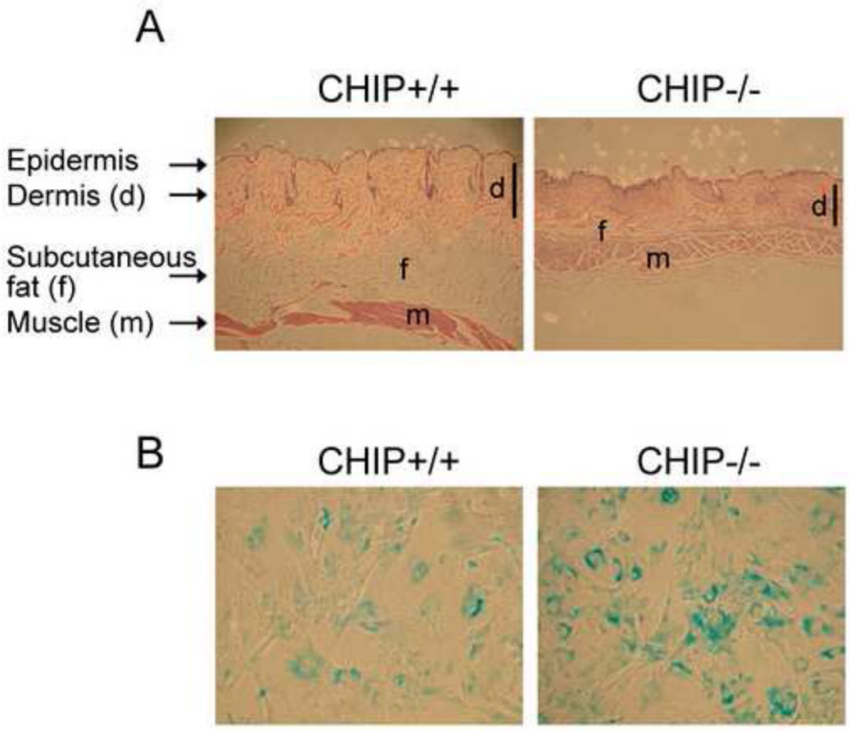

Figure 2. Dermal thickness analysis and SA-β-gal activity as a measure of aging

A. Representative histological sections of skin from CHIP-/- and CHIP+/+ mice at 12 month of age (original magnification 200×). CHIP-/- mice show a greatly reduced dermis layer in the skin compared with CHIP+/+ mice. The black bar indicates the dermis layer within the skin section. (Dermis; d, Subcutaneous fat; f, Muscle; m) B. Representative images of SA-β-gal staining in CHIP-/- and CHIP+/+ MEFs at P8 (original magnification 200×). Blue staining in the cells indicates SA-β-gal activity. Figure 2 is modified from Min JN et al., Mol. Cell. Biol., 2008.

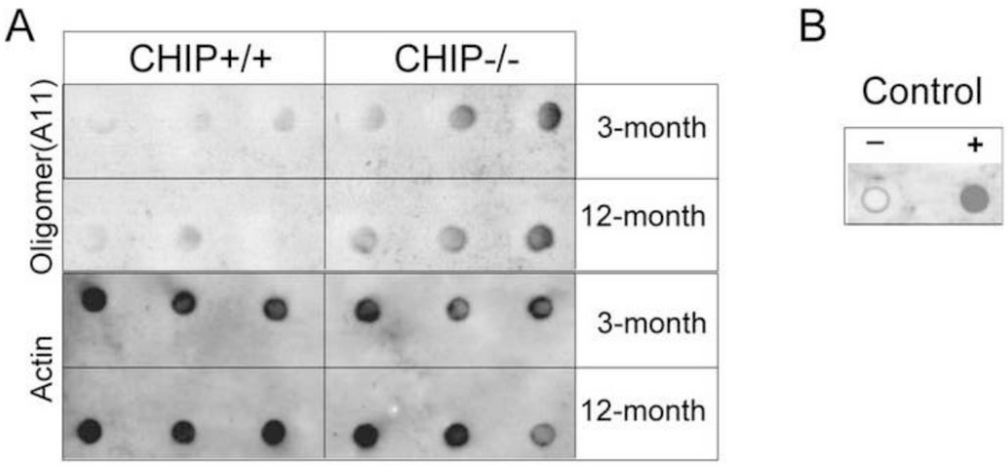

Figure 3. Dot blot analysis for oligomer protein in brain tissues

A. Expression of misfolded oligomer proteins in brain tissues (10ug of protein) obtained from indicated genotype and age groups as measured by a dot-blot analysis using the anti-oligomer (A11) antibody. Actin was used as a loading control. B. Dot blot analysis showing positive (+) and negative (-) controls for the anti-oligomer antibody (see text). Figure 3 is modified from Min JN et al., Mol. Cell. Biol., 2008. Since the A11 antibody is directed against a common oligomeric conformation, identification of the specific oligomerized protein(s) in this assay is not possible.

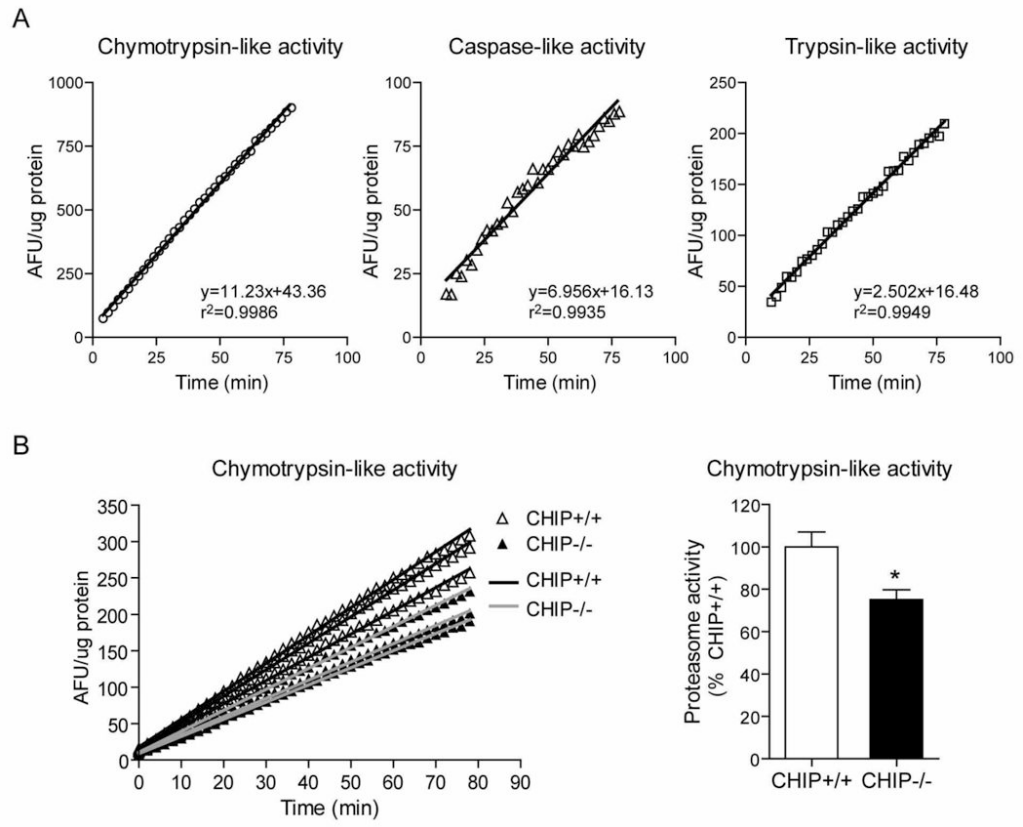

Figure 4. 26S proteasome activity assay

A. Representative graphs and linear regressions for proteasome assays using three different fluorogenic substrates. B. Left panel; Graph for chymotrypsin-like activity in a liver sample from CHIP+/+ and CHIP-/- mice at 12 months of age. Data from each mouse sample (n=3 per genotype) are shown in graph and individual line generated from linear regression analyses from each data set. Right panel; Percentile of chymotrypsin-like activity (slopes from the graph on the left) was measured relative to the activity (slopes) in CHIP+/+ mice. Data shown were obtained from left graph and indicated by mean ± SEM. *, $p<0.05$ (Student's *t*- test). Figure 4B. is modified from Min JN et al., Mol. Cell. Biol., 2008.